

Polarization Message Encoding through Vectorial Chaos Synchronization in Vertical-Cavity Surface-Emitting Lasers

Alessandro Scirè,¹ Josep Mulet,¹ Claudio R. Mirasso,² Jan Danckaert,^{1,3} and Maxi San Miguel¹

¹*Instituto Mediterráneo de Estudios Avanzados (IMEDEA), Consejo Superior de Investigaciones Científicas–Universitat de les Illes Balears, Campus Universitat Illes Balears, E-07071 Palma de Mallorca, Spain*

²*Departament de Física, Universitat de les Illes Balears. E-07071 Palma de Mallorca, Spain.*

³*Vrije Universiteit Brussel, Department of Applied Physics and Photonics (TW - TONA) Pleinlaan 2, B-1050 Brussels, Belgium*
(Received 22 August 2002; published 18 March 2003)

We show that self-pulsating vertical-cavity surface-emitting lasers can exhibit vectorial chaos, i.e., chaos in both intensity and polarization. The achievable synchronization degree of two such lasers is high when using a continuous control scheme and unidirectional coupling. We propose a novel encryption scheme, where the phase of the vectorial field is modulated. Therefore, the total intensity of these lasers remains synchronized while the intensities in the polarization modes (de)synchronize following the phase modulation at a ps time scale. This technique allows for transmission of secure data at high bit rates that are not limited by the relaxation oscillation frequency.

DOI: 10.1103/PhysRevLett.90.113901

PACS numbers: 42.60.Mi, 42.55.Px, 42.62.-b, 42.65.Sf

Systems with vectorial degrees of freedom, as well as those described by scalar variables, exhibit interesting dynamical regimes such as frequency locking and chaos. In the field of optics, the vectorial character of the light is given by the two independent polarization components of the electric field. The dynamics of these polarization components has been studied for many optical systems, including nonlinear devices [1], gas, and semiconductor lasers [2]. Although unstable behaviors such as chaotic emission are often considered undesirable, the synchronization properties of chaotic systems have received much attention in the last decade motivated by the potential application in secure optical communications systems [3–7]. To this purpose also the polarization of the laser light revealed to be useful [8]. Vertical-cavity surface-emitting lasers (VCSELs) [9] are semiconductor lasers characterized by light emission orthogonal to the active layer, and showing substantial practical advantages in comparison to the more conventional edge-emitting lasers (EELs), for example, their compactness, superior beam quality, low threshold currents, and high efficiencies. From the nonlinear dynamics and laser physics point of view, VCSELs differ in one crucial aspect from standard EELs: the polarization state of the light emitted by a VCSEL is not fixed *a priori* by the device's almost perfect cylindrical symmetry. Therefore, a rich dynamical polarization behavior is encountered in these devices [10,11]. Also self-pulsations have been experimentally demonstrated in a solitary VCSEL [12]. These self-pulsations in combination with the polarization degree of freedom allow, under certain operation conditions, for the existence of chaos [13] without the need of any external perturbation or feedback scheme. As this chaos involves both intensity and polarization, we call it *vectorial chaos*. In this Letter we investigate the synchronization properties of the vectorial chaos present in a VCSEL, showing that a particular transition from quasi to fully synchro-

nized chaotic states is possible. We also demonstrate theoretically that this transition can be exploited in secure communication applications, increasing the security level and the transmission velocity, and without the need of inducing chaos through external perturbations (e.g., feedback or injection).

We consider master and slave VCSEL where the active region is surrounded by a zone with saturable absorber. The VCSEL dynamics can be described [13] in the framework of the standard spin flip model [14] for the polarization dynamics, combined with the well-known Yamada model [15] for semiconductor laser in the presence of a saturable absorber. The rate equations describing the dynamical evolution of the slowly varying complex amplitudes of the two circularly polarized optical fields $F_{\pm M,S}$ in the Master and Slave lasers, respectively, can be written concisely as [13]

$$\dot{F}_{\pm}^M = \mathcal{F}_{\pm}(D_{1,2}^M, d_{1,2}^M)F_{\pm}^M + (\gamma_a + i\gamma_p)F_{\mp}^M + f_{\pm}^M(t), \quad (1)$$

$$\dot{F}_{\pm}^S = \mathcal{F}_{\pm}(D_{1,2}^S, d_{1,2}^S)F_{\pm}^S + (\gamma_a + i\gamma_p)F_{\mp}^S + f_{\pm}^S(t) + \Gamma(F_{\pm}^M + H_0 e^{i\phi} F_{\pm}^S). \quad (2)$$

As in any semiconductor laser, the field equations depend on the carrier populations and henceforth Eqs. (1) and (2) have to be complemented with carrier equations for $D_{1,2 M,S}$, the total carrier inversion between the conduction and valence bands (the indices 1 and 2 stand for the pumped and absorbing regions in each laser, consistently with the Yamada model, as reported in [13]). Furthermore, within the SFM description of VCSELs there is a dynamical dependence on $d_{1,2 M,S}$, the differences of the carrier populations with opposite spin orientations. The full set of equations can be found in Ref. [13]. The optical fields F_{\pm} in each laser are coupled through phase and amplitude anisotropies γ_p and γ_a [10]. Small values of γ_a are usually encountered in VCSELs

and, since our results only weakly depend on this parameter, we set $\gamma_a = 0$. The spontaneous emission noise terms $f_{\pm M, S}$ contain independent complex Gaussian random numbers with zero mean and delta correlation [16]. Finally, through the last term in Eq. (2) we describe unidirectional coupling (see Fig. 1) of the Master laser to the Slave one, where Γ is the overall injection attenuation, and H_0 and ϕ the attenuation and dephasing acquired in the feedback loop. All the numerical simulations were performed with the parameters given in [13], except for the phase anisotropy which takes the value $\gamma_p = 25 \text{ ns}^{-1}$.

One of the dynamical regimes exhibited by the master laser is a region of chaotic behavior, subsequent to a birefringence-induced Hopf bifurcation [13]. In the rest of this Letter we concentrate on this particular regime. To visualize the complex dynamics that arise in this region, we show in Fig. 2 the total intensity time trace together with the time evolution of two of the projections of the vector electric field onto the Poincaré sphere. These projections are shown in terms of the normalized Stokes parameters S_1/S_0 , S_2/S_0 , and S_3/S_0 [16]. It can be seen that the electric field is a vectorial magnitude changing its polarization state over a chaotic attractor in the Poincaré sphere. At the same time, the amplitude of the electric-field vector evolves chaotically, showing that chaos is present in both polarization and in the total emitted intensity. We have checked that the dynamics is indeed chaotic by computing the largest of the Lyapounov exponents which is clearly positive for the parameters chosen.

We next consider the synchronization properties of the coupled system. The simplest coupling scheme between two such systems is the direct coupling [4], i.e., $H_0 = 0$ in Eq. (2). However, we find that in such a standard scheme only an intermittent synchronization can be achieved that is not robust against introduction of noise and/or parameter mismatches. Therefore, we use instead a continuous control scheme coupling [17] (CCS), schematically shown in Fig. 1, that has proven to yield more robust synchronization in EELs [18]. For simplicity, we assume that the M and S systems are twin systems (same values of all

parameters). If we set the phase in the feedback loop to $\phi = \pi$ and increase Γ , we find that after a certain critical value $\Gamma = \Gamma_c$ the trajectories of the M and S systems synchronize. To quantitatively express the degree of synchronization we generalize the scalar mean relative error [18] to the circular components of the field

$$\sigma_{\pm} = \frac{\langle |F_{\pm}^M - F_{\pm}^S| \rangle}{\langle |F_{\pm}^M| \rangle}, \quad (3)$$

where $\langle \cdot \rangle$ means temporal average. In Fig. 3 we show the transition of the coupled system from an unsynchronized ($\sigma_{\pm} \sim 1$) to a synchronized state ($\sigma_{\pm} \ll 1$). We disregard the flight time T_f from the Master to the Slave laser, since the slave system dynamics remains invariant under a time translation $t - T_f$ by t . A high quality synchronization can thus be reached using identical devices and under realistic noise conditions. The accuracy needed to fulfill the condition $\phi = \pi$ has been already discussed in the literature [18] and is found, in general, to be critical. This is also the case for our VCSEL system. The difference $F_{\pm}^M - F_{\pm}^S$ requires coherent field superposition (with π phase shift) at a beam combiner; therefore, a suitable active control of the path length must be introduced in the setup, since, for efficient synchronization, the residual phase error must not exceed a few degrees. The accuracy level needed for this practical requirement is of the same order as in coherent detection or interferometry.

The synchronization method just described can be exploited in a secure communication scheme, taking advantage of the vectorial nature of the chaotic field. Similar to what has been demonstrated in a fiber ring laser [8], the information can be encoded in the polarization state of the emitted light, leaving the average total intensity unaffected. For this purpose, we introduce a

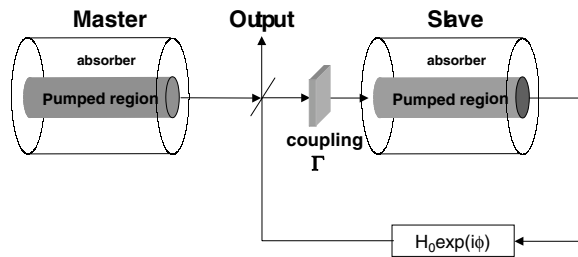


FIG. 1. Sketch of the continuous control synchronization scheme needed to achieve synchronization between two vectorially chaotic VCSELs. The passive components are meant to be polarization insensitive.

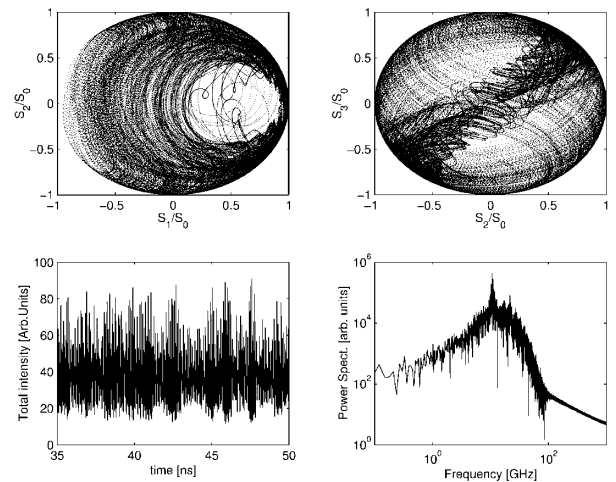


FIG. 2. The upper panels show the normalized Stokes parameter phase space, while the lower ones show the time evolution of the total intensity (left) and the power spectrum (right). Parameter values are the same as in Ref. [13], except for $\gamma_p = 25 \text{ ns}^{-1}$.

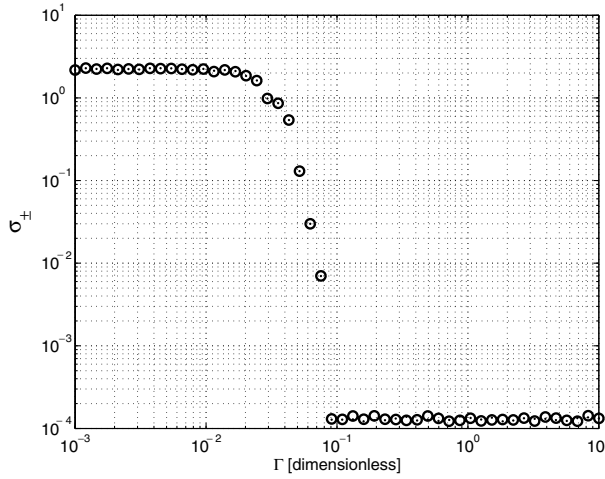


FIG. 3. Synchronization error (σ_+ , circles and σ_- , dots) as a function of the coupling strength Γ . The transition from an unsynchronized ($\sigma_{\pm} \sim 1$) state to synchronization takes place at $\Gamma \sim 0.08$. Noise effects were included in the simulations as in [16] setting the lower limit of the synchronization error (noise floor).

polarization modulator at the output of the Master laser. In the “on” state for which we assume the bit “1”, the polarization modulator changes the phase relation between the two orthogonal polarizations, which is invisible in the total emitted intensity. The “off” state (bit “0”) leaves the emitted field unaffected. The demodulation scheme is a standard on-off chaos shift keying (OCSK) [18,19]: the Slave synchronizes (desynchronizes) to the received signal when a 0 (1) bit is received (see Fig. 4). It is interesting to note that, while the x and y polarizations (de)synchronize following the phase modulation, the total intensity of the two lasers remains synchronized all the time except for small bursts (see Fig. 5). Another interesting aspect is that the synchronization is much faster than the typical ns time scale present in conventional chaotic semiconductor lasers [18] (see Fig. 4). To quantify the synchronization response we have calculated the synchronization time, i.e., the time it takes the system to resynchronize once the relative phase between the two polarization components is set back to zero. The results are shown in Fig. 6, where it can be seen that, for our parameters values, the mean synchronization time is about 1.35 ps, with a statistical distribution originated by the chaotic nature of the fluctuations, when passing from a desynchronized to a synchronized state. For typical VCSEL parameters vectorial chaos synchronization could allow for encoding rates much faster than any other traditional CSK scheme. Only if the total intensity synchronization is lost our system acts like the traditional CSK, recovering the full synchronization with a characteristic time of the order of the inverse of the relaxation oscillation frequency (about 10.5 GHz for our parameters). The very fast synchronization demonstrated here follows from the fact that our

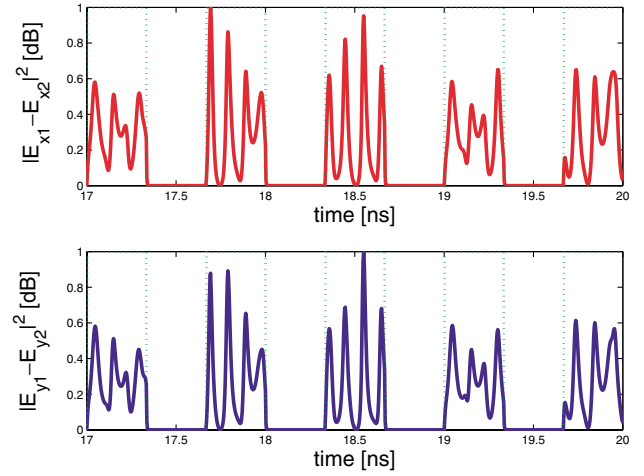


FIG. 4 (color online). Bit recovery: as the phase between the two polarization components in the input signal is modulated between 0 and π at the times shown by the vertical dashed lines, the information is recovered at the “Output” shown in Fig. 1, in both x and y polarizations. For π phase shift both polarizations are desynchronized, while they resynchronize very rapidly as the phase is set back to 0. The total intensity (not shown) remains synchronized all the time. $\Gamma = 0.9$, and the modulation bit frequency shown here is 3 Gbits/s, but can be increased up to 100 Gbits/s.

systems remain in a state of partial synchronization all the time: the total intensity remains synchronized, while the polarization components (de)synchronize following the phase modulation. Reestablishing the

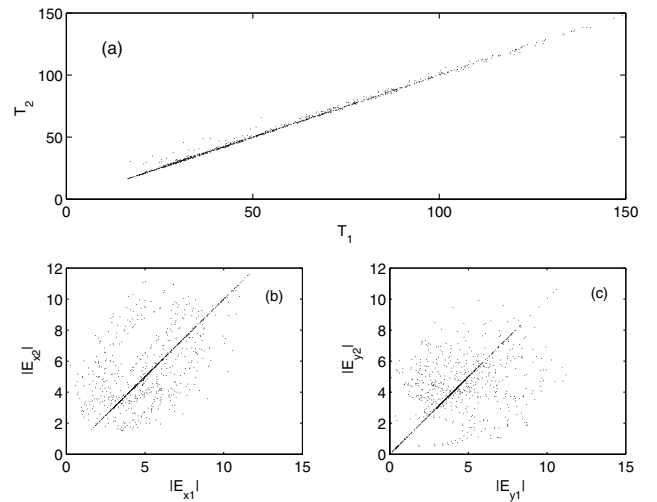


FIG. 5. Synchronization diagrams corresponding to Fig. 4: (a) the total intensities of the Master and Slave sources (T_1 and T_2 , respectively) keep synchronized all the time except for small bursts and a small variation in the cross correlation between T_1 and T_2 : 0.998 (0.996) when 0 (1) is transmitted. The respective x (b) and y (c) polarizations (de)synchronize when a 0 (1) is received. The units are dimensionless, $\Gamma = 0.9$, and the bit frequency is 3 Gbits/s.

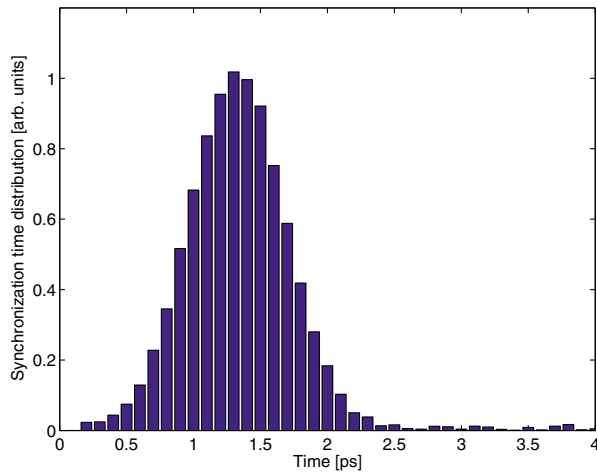


FIG. 6 (color online). Probability distribution of the synchronization time calculated as the time at which the difference between the two fields drop below the 10% of the mean emitted power. Noise effects were included in the simulations as in [16].

synchronization of the polarization components only involves the phases of the fields and not their intensities. Henceforth our polarization encoding is not limited by the relaxation oscillation frequency.

In conclusion, we have discussed the synchronization properties of the vectorial chaos generated by a chaotic VCSEL. A main difference of these devices with respect to conventional edge-emitting lasers is that, due to the polarization degree of freedom, chaos in both intensity and polarization can be obtained without any external perturbation or feedback scheme. We find that two identical systems can synchronize when using a continuous control scheme in the receiver. Moreover, such a chaos can completely synchronize and partially desynchronize in a state where the two systems share the same total chaotic intensity, while they show very different polarization fluctuations. These two states can be exploited in a novel encryption scheme, where the information is encoded in the phase variables rather than in the intensity of the carrier light beam. This encoding scheme has two major advantages as compared to traditional ones. On the one hand, as the information is added in the phase, the average total intensity remains unaffected, a guarantee against unwanted eavesdropper attacks. On the other hand, our synchronization scheme is shown to be very fast, with a synchronization time scale of few picoseconds.

This work has been funded by the European Commission through VISTA HPRN-CT-2000-00034, OCCULT Project No. IST-2000-29683, COST268 action, and the Spanish MCyT under Project No. BFM2000-1108, MCyT and Feder SINFIBIO BFM 2001-0341-C02-01. A. S. acknowledges Marie Curie IF

MCFI-2000-00617, J. D. acknowledges funding project support from FWO (Fund for Scientific Research, Belgium). The authors thank Dr. M. Matias (IMEDEA) for helping in the Lyapunov exponents calculation.

-
- [1] Special issue on polarization effects in lasers and spectroscopy, edited by N.B. Abraham and G.M. Stephan [Quantum Semiclass. Opt. **10** (1998)]; M. Hoyuelos, P. Colet, M. San Miguel, and D. Walgraef, Phys. Rev. E **58**, 2992 (1998).
 - [2] N.B. Abraham, E. Arimondo, and M. San Miguel, Opt. Commun. **117**, 344 (1995); **117**, 121 (E) (1995); **117**, 168 (1995); C. Serrat, A. Kul'minskii, R. Vilaseca, and R. Corbalán, Opt. Lett. **20**, 1353 (1995); A. Kul'minskii, R. Vilaseca, and R. Corbalán, Opt. Lett. **20**, 2390 (1995); M. San Miguel, Phys. Rev. Lett. **75**, 425 (1995); C. A. Sharma, M. A. van Eijkelenborg, J. P. Woerdman, and M. San Miguel, Opt. Commun. **138**, 305 (1997); A. Kul'minskii, R. Vilaseca, R. Corbalán, and N.B. Abraham, Phys. Rev. A **62**, 033818 (2000); Hernandez-Garcia, M. Hoyuelos, P. Colet, and M. San Miguel, Phys. Rev. Lett. **85**, 744 (2000).
 - [3] P. Colet and R. Roy, Opt. Lett. **19**, 2056 (1994).
 - [4] C. R. Mirasso, P. Colet, and P. Garcia-Fernandez, IEEE Photonics Technol. Lett. **8**, 299 (1996).
 - [5] G. Van Wiggeren and R. Roy, Science **279**, 1198 (1998).
 - [6] J. P. Goedgebuer, L. Larger, and H. Porte, Phys. Rev. Lett. **80**, 2249 (1998).
 - [7] S. Tang and J. M. Liu, Opt. Lett. **26**, 596 (2001).
 - [8] G. Van Wiggeren and R. Roy, Phys. Rev. Lett. **88**, 097903 (2002).
 - [9] K. J. Ebeling, in *Semiconductor Quantum Optoelectronics: from Quantum Physics to Smart Devices, Proceedings of the Fiftieth Scottish Summer School in Physics, St. Andrews, 1998*, edited by A. Miller, M. Ebrahimzadeh, and D. M. Finlayson (Institute of Physics, Bristol, 1999).
 - [10] M. San Miguel, in *Semiconductor Quantum Optoelectronics: from Quantum Physics to Smart Devices* (Ref. [9]), pp. 339–366.
 - [11] G. Verschaffelt *et al.*, Opto-Electron. Rev. **9**, 257 (2001).
 - [12] M. Willemsen, M. P. van Exter, and J. P. Woerdman, Appl. Phys. Lett. **77**, 3514 (2000).
 - [13] A. Scirè, J. Mulet, C. R. Mirasso, and M. San Miguel, Opt. Lett. **27**, 391 (2002).
 - [14] M. San Miguel, Q. Feng, and J. V. Moloney, Phys. Rev. A **52**, 1728 (1995).
 - [15] M. Yamada, IEEE J. Quantum Electron. **29**, 1330 (1993).
 - [16] J. Mulet, C. R. Mirasso, and M. San Miguel, Phys. Rev. A **64**, 023817 (2001).
 - [17] T. Kapitaniak, Phys. Rev. E **50**, 1642 (1994).
 - [18] V. Annovazzi-Lodi, S. Donati, and A. Scirè, IEEE J. Quantum Electron. **32**, 953 (1996); **33**, 953 (1997).
 - [19] J. B. Cuenot, L. Larger, J. P. Goedgebuer, and W. T. Rhodes, IEEE J. Quantum Electron. **37**, 849 (2001).